Received: 9 February 2018 | Revised: 24 March 2018 | Accepted: 27 March 2018

DOI: 10.1111/cas.13599

ORIGINAL ARTICLE

WILEY Cancer Science

Enhancer of zeste homolog 2 promotes cisplatin resistance by reducing cellular platinum accumulation

Si Sun | Simei Zhao | Qiang Yang | Wenwen Wang | E Cai | Yiping Wen | Lili Yu | Zehua Wang | Jing Cai

Department of Obstetrics and Gynecology, Union Hospital, Tongji Medical College, Huazhong University of Science and Technology, Wuhan, China

Correspondence
Zehua Wang and Jing Cai, Department of Obstetrics and Gynecology, Union Hospital, Tongji Medical College, Huazhong University of Science and Technology, Wuhan, China.
Emails: zehuawang@163.net and caijingmmm@hotmail.com

Funding information
National Natural Science Foundation of China, Grant/Award Number: 81372807, 81572571, 81702570

Enhancer of zeste homolog 2 (EZH2), which is overexpressed in a wide range of tumors, contributes to ovarian cancer malignancy in several different ways. We aimed to illustrate the role of EZH2 in ovarian cancer cisplatin resistance and to identify possible underlying mechanisms of this role that may provide a rationale for targeting EZH2 in cancer treatment. Here, we present data indicating that EZH2 overexpression is associated with cisplatin resistance and intracellular platinum drug accumulation. Measurements of EZH2 in 84 ovarian cancer patients suggested that patients with high EZH2 levels tend to have poor responses to cisplatin. The EZH2 level progressively increased in cells receiving repeated cisplatin exposure. Down-regulation of EZH2 not only sensitized cellular reactions to cisplatin and increased cellular platinum accumulation when cells were exposed to both cisplatin and BOD-IPY-Pt (a fluorescent cisplatin complex) but also protected copper transporter 1, a high-affinity copper transporter closely related to cisplatin resistance, from cisplatin-induced proteasomal degradation. Overall, these findings identify a new mechanism that expands the unrecognized role of EZH2 in ovarian cancer cisplatin resistance.

KEYWORDS
cisplatin resistance, copper transporter 1, enhancer of zeste homolog 2, ovarian cancer, platinum accumulation

1 | INTRODUCTION

Cisplatin (cDDP) has been widely used in ovarian cancer treatment since the late 1970s. However, nearly 70% of ovarian cancer patients develop cDDP resistance, which greatly limits the chemotherapeutic effect of this drug.[1] Drug modification, combination therapy, and novel drug delivery systems have been applied to circumvent cDDP resistance for greater clinical benefit. Cisplatin analogs such as carboplatin and oxaliplatin produce excellent clinical anticancer effects, but patients eventually develop cross-resistance to these drugs as well.[2] Therefore, understanding the development of cDDP resistance is vital in identifying new treatment strategies.

Until now, the mechanisms for how ovarian cancer develops resistance to cDDP have been characterized by decreased cellular platinum accumulation, increased platinum-DNA damage tolerance, increased platinum detoxication, impaired apoptosis initiation, and enhanced DNA damage repair.[3] Multiple independent research groups in earlier reports identified that reduced intracellular drug accumulation rendered ovarian cancer, non-small-cell lung cancer, prostatic cancer, hepatoma cancer, cervical cancer, and colorectal cancer cell lines resistant to cDDP.[4] Recent studies have provided further evidence of the association between cancer tissue platinum concentration and chemotherapy response in muscle-invasive

Si Sun and Simei Zhao contributed equally to the work.

bladder cancer and non-small-cell lung cancer.[5,6] This evidence suggests that reduced platinum accumulation is an important mechanism of platinum resistance.

The enhancer of zest homolog 2 (EZH2) is the catalytic component of the polycomb repressive complex 2 (PRC2), which can transfer methyl groups to histone 3 on lysine 27 (H3K27Me3) by the SET domain to repress gene transcription through DNA methylation.[7] In normal biological processes, the expression of EZH2 is silenced after it fulfills its duty in embryonic development. However, the overexpression of EZH2 in cancer compared to normal tissue has brought this protein to the attention of oncologists.[8,9] Previous studies investigating the basic genetic landscape of EZH2 in cancers and how it promotes malignancy revealed that EZH2 is involved in a wide range of cancer-associated processes. In ovarian cancer, mounting evidence suggests that EZH2 correlates with shortened overall survival in ovarian cancer patients,[10] induces the epigenetic repression of tumor-suppressor genes,[11] enhances the proliferation, migration, and invasion ability of ovarian cancer cells in vivo and in vitro,[12] participates in maintaining the ovarian cancer epithelial phenotype, and represents a new characteristic of the ovarian cancer stem cell-like population.[13]

In this paper, we explored the relationship between EZH2 and cDDP resistance in ovarian cancer. This analysis was achieved by establishing the correlation between EZH2 and cDDP resistance in cellular models and patient tissue samples. In addition, we examined the effect of EZH2 on cellular platinum accumulation. Finally, we studied the reaction of copper transporter 1 (CTR1), a high-affinity copper influx transporter closely related to platinum resistance, to cDDP in ovarian cancer cells and analyzed how EZH2 is involved in the interaction between cDDP and CTR1.

2 | MATERIALS AND METHODS

2.1 | Human ovarian cancer tissues and sample preparation

Archival paraffin-embedded tissue blocks were obtained from the tissue bank of the Department of Obstetrics and Gynecology, Union Hospital, Tongji Medical College, at the Huazhong University of Science and Technology (Wuhan, China). The study protocol was approved by the Wuhan Union Hospital Institutional Review Board. All patients gave written consent before enrollment. Patients with pathologically confirmed epithelial ovarian cancer who underwent primary surgery followed by platinum-based adjuvant chemotherapy between August 2008 and October 2015 were enrolled. Patients who received prior chemotherapy or radiotherapy treatment were excluded. For adjuvant chemotherapy, a regimen of carboplatin (400 mg, i.v.; Qilu Pharma, Shandong, China) combined with liposomal paclitaxel (135-175 mg/m^2, i.v.; Luye Pharma Group, Jiangsu, China) every 3 weeks for six cycles was used.[14] Chemoresistance is characterized by tumors that show no response to chemotherapy (stable disease), progression during chemotherapy, or chemotherapy relapse within 6 months of the completion of primary chemotherapy.[9] A total of 64 surgery specimens, including 45 chemosensitive and 19 chemoresistant tumors, were enrolled, and their basic characteristics are shown in Table 1.

2.2 | Tissue microarray and immunohistochemistry

Paraffin-embedded tissues were used for the tissue microarray. According to the results from matched H&E control staining, tissue cylinders of 2 mm in diameter were sampled from areas containing the most representative malignant cells by a MiniCore Control Station (Alphelys Sarl, France). Microarray blocks were assembled by a tissue arrayer (Beecher Instruments, Sun Prairie, WI, USA) and were cut into 4-μm-thick sections for subsequent immunohistochemical staining for EZH2. The immunohistochemical assays were carried out by using a Histostain SP Kit (ZSGB-Bio, Beijing, China) according to the manufacturer's instructions. In brief, slides were baked at 60°C for 1 hour, dewaxed in xylene three times (5 min/wash), and rehydrated through descending graded ethanol (100%, 95%, and 70%) washes, ending with a water wash. The slides were then rinsed in citrate (pH 6.0) for antigen retrieval through microwave irradiation followed by the procedures outlined in the Histostain SP Kit protocol. Anti-EZH2 antibody (1:100; Cell Signaling Technology, USA) was applied at 4°C in a humidified atmosphere overnight. The bound antibody was detected using a DAB Kit (ZSGB-Bio). The images were documented using a fluorescence microscope (IX71; Olympus, Japan).

Two investigators blinded to patient information and sample data evaluated the EZH2 expression independently. Discrepancies were solved by discussion or by consulting a third pathologist. A semi-quantitative scale was used to assess the immunostaining of EZH2 and CTR1. A staining score (0-9) was calculated by multiplying the staining intensity score (0, negative; 1, light yellow; 2, yellow; and 3, dark brown) with the positive proportion of cells (0, 0%; 1, <25%; 2, 25%-50%; 3, 50%-75%; 4, >75%).

TABLE 1 Basic characteristics of 84 ovarian cancer patients

Characteristics	n (%)
Age, years; median (range)	52 (32-72)
Histologic type	
High-grade serous carcinoma	50 (78.10)
Low-grade serous carcinoma	4 (0.65)
Mucinous carcinoma	3 (0.55)
Endometrioid carcinoma	4 (0.65)
Clear cell carcinoma	3 (0.55)
FIGO stage	
I-II	16 (25.00)
III-IV	48 (75.00)
Chemotherapy response	
Chemosensitive	45 (70.31)
Chemoresistant	19 (29.69)

FIGO, International Federation of Gynecology and Obstetrics.

2.3 | Cell culture and drugs

The A2780 and ES2 human ovarian cancer cell lines were purchased from the China Center for Type Culture Collection (China) and validated by short tandem repeat profiling (Biowing Applied Biotechnology, Shanghai, China). The cDDP-resistant cell lines A2780C12 and ES2C12 were generated by exposing the parent cells to cDDP with increasing drug concentrations for 12 cycles. Cells were grown in DMEM supplemented with 10% FBS in a humidified incubator with 5% CO_2 at 37°C. Cisplatin was purchased from Sigma (USA). BODIPY-Pt was a gift from Dr. Wenliang Li (National Engineering Laboratory for Druggable Gene and Protein Screening, School of Life Science, Northeast Normal University, Changchun, China). 3-Deazaneplanocin A (DZNEP), GSK126, cycloheximide (CHX), and MG132 were purchased from Cayman Chemical, USA.

2.4 | Cell transfection

Lentiviral EZH2 specific shRNA (shEZH2) and a scrambled control shRNA (shNC) were synthesized by GenePharma (Suzhou, China). The sequences were: shEZH2, 5′-GCAACACCCAACACTTATAAG-3′; and shNC, 5′-TTCTCCGAACGTGTCACGTTTC-3′. Small interfering RNAs specific for EZH2 and a scrambled control were synthesized by Genechem (Shanghai, China). The sequences were: siEZH2, 5′-TTGCCTTCTCACCAGCTGC-3′; and siNC, 5′-TTCTCCGAACGTG TCACGT-3′. The EZH2 overexpression plasmid was constructed in our laboratory as previously described (GV166-EZH2 plasmid).[9] Stable transfection of the EZH2 knockdown lentivirus and EZH2 overexpression plasmid was undertaken as previously described.[9] The siRNA transient transfections were carried out using Lipofectamine 2000 (Invitrogen, Carlsbad, CA, USA).

2.5 | Real-time PCR

RNA extraction and real-time PCR were carried out as previously described.[15] The sequences of the primers were: EZH2 forward, 5′-TTGTTGGCGGAAGCGTGTAAAATC-3′ and reverse, 5′-TCCCTAG TCCCGCGCAATGAGC-3′; and β-actin forward, 5′-GCCAACAC AGTGCTGTCTGG-3′ and reverse, 5′- GCTCAGGAGGAGCAATG ATCTTG-3′. Standard curves were established prior to the PCR reactions to confirm the amplification efficiencies to be approximately 100%. The PCR reactions were undertaken using the two-step thermal cycling method: 95°C for 1 minute, 40 cycles at 95°C for 20 seconds, 60°C for 20 seconds, and 70°C for 10 seconds. The EZH2 expression level was normalized to β-actin and calculated using the $2^{-\Delta\Delta Ct}$ method. Each experiment was carried out in triplicate at least three times.

2.6 | Western blot analysis

Cell lysate preparation and Western blotting were undertaken as previously described.[16] The primary antibodies used were EZH2 (1:1000; Cell Signaling Technology), CTR1 (1:500; Santa Cruz Technology), CTR2 (1:500; Novus Biologicals), ATP7A (1:500; Santa Cruz Technology), ATP7B (1:500 Santa Cruz Biotechnology), H3K27Me3 (1:1000; Active Motif), H3 (1:1000; Active Motif), mono-Ub (1:1000; VIVA Bioscience), poly-Ub (1:200; Santa Cruz Biotechnology), and β-actin (1:5000; Proteintech). The results were visualized using an enhanced chemiluminescence kit (Bio-Rad) and scanned using a Molecular Imager Chemi-Doc XRS+ system (Bio-Rad). The relative expression of EZH2 and CTR1 to β-actin was calculated by quantifying the gray values using Bio-Rad Quantity One software.

2.7 | Cytotoxicity assays

Cells (4000 per well) were seeded in 96-well plates and treated with a range of cDDP (0-32 μmol/L) for 72 hours. Viability was assayed by MTS (Sigma) according the manufacturer's instruction.

2.8 | Colony formation assay

Cells (1000 per well) were seeded and incubated with different concentrations of cDDP (0-8 μmol/L) for 24 hours and change to drug-free media until visible colonies appeared. The colonies were fixed with 4% formaldehyde, stained with crystal violet, counted, and photographed. Clusters of more than 50 cells were considered a colony.

2.9 | Determination of cellular platinum accumulation, uptake, and efflux

Cell pellets were harvested after 12 hours of exposure to 30 μmol/L cDDP. The pellets were divided into halves, one for protein determination using a BCA Protein Assay Reagent Kit (Bio-Rad), and the other was kept frozen until submission for flame atomic absorption spectroscopy (FAAS) analysis as previously described.[17] To examine the influx rate, cells were exposed to 500 μmol/L cDDP and harvested at different time points. To examine cDDP efflux, cells were exposed to 500 μmol/L cDDP for 10 minutes (time 0), washed with cold PBS and kept in drug-free medium for 10, 20, and 30 minutes. Cells collected at each time point were processed as described above.

2.10 | Immunofluorescence

Cells were seeded on coverslips 24 hours before treating with 20 μmol/L BODIPY-Pt for 1-8 hours. After treatment, cells were fixed, permeabilized and blocked. The blocked cells were then incubated with anti-CTR1 (1:100; Santa Cruz Biotechnology) overnight at 4°C, incubated with goat-anti-rabbit IgG Alexia (1:100; EarthOX) for 1 hour. Nuclear staining was carried out using DAPI (100 ng/mL; ATT Bioquest). An A1-Si confocal laser-scanning microscope (Nikon), ImageJ 1.50i/Java 1.6.0 software (NIH, Bethesda, MD, USA), and CoLocalizer Pro software (Tokyo, Japan) were used to process the images.

2.11 | Protein stability assay

Cells were treated with 20 μmol/L CHX for 3, 6, or 9 hours and harvested for Western blot analysis. The levels of CTR1 at each time point were measured by the gray value, which was adjusted according to β-actin and then normalized to the DMSO control.

2.12 | Immunoprecipitation

Cells were pre-incubated with 20 μmol/L MG132 for 4 hours and then treated with saline or 30 μmol/L cDDP for 12 hours. After treatment, the cells were harvested and lysed as previously described; 100 μL lysates were used as the input. The remaining lysates were precleared with 20 μL Protein A/G beads (Santa Cruz Biotechnology) for 1 hour. After centrifugation, the supernatants were removed and incubated with anti-CTR1 (1:100; Santa Cruz Biotechnology) or anti-Flag (1:100; Sigma) and IgG (1:100; Proteintech) for 2 hours. Protein A/G beads (20 μL) were then added to each sample for overnight rotation. The beads were washed three times with cold lysis buffer and subjected to Western blot analysis. A fraction of the anti-Flag incubated beads was also submitted for mass spectrometry.

2.13 | Statistical analysis

Student's *t*-test and the Mann-Whitney test were performed with Prism 6.0 software (GraphPad Software, San Diego, CA, USA). *P*-values <.05 were considered statistically significant.

3 | RESULTS

3.1 | Enhancer of zeste homolog 2 is associated with cDDP resistance in ovarian cancer

To verify the relationship between EZH2 and cDDP resistance, we first compared EZH2 expression in chemosensitive vs chemoresistant tumors. As shown in Figure 1(A), the tissue microarray and immunohistochemical assays revealed that EZH2 staining in the chemoresistant group was much stronger than in the chemosensitive group. As CTR1 was a prognostic marker for ovarian cancer chemotherapy response, as assessed in our previous meta-analysis,[18] we also included the measurement of CTR1 using our own cohort to validate this previous conclusion. As expected, the chemosensitive group showed stronger CTR1 staining. We undertook a correlation analysis between EZH2 and CTR1 levels but we did not find any evidence of correlation (Figure S1; Pearson $R = -.1301$, $P = .326$). Next, we generated two cDDP-resistant cell sublines, A2780C12 and ES2C12, by exposing A2780 and ES2 parental cells to 12 cycles of cDDP treatment, respectively (Figure 1B). We observed a progressively increased expression of EZH2 and its substrate H3K27Me3 in both cell lines during cDDP resistance induction (Figure 1C). To verify the contribution of EZH2 to cDDP resistance in ovarian cancer cells, A2780 and ES2 were stably transfected with EZH2 inhibition plasmid shEZH2, ES2 was stably transfected with EZH2 overexpression plasmid (Figure 1D,E). The downregulation of EZH2 dramatically increased the sensitivity of A2780 and ES2 cells to cDDP, whereas overexpression of EZH2 contributed to cDDP resistance (Figure 1F).

3.2 | Enhancer of zeste homolog 2 affects intracellular platinum accumulation

In a previous study, we observed increased cDDP accumulation accompanied by a decrease in EZH2 in mouse s.c. xenografts after cDDP and let-7e agomir combination treatment.[19] To determine whether EZH2 affects platinum accumulation in ovarian cancer cells, we analyzed the platinum content of cells with different EZH2 levels. We found that platinum content was significantly higher in the EZH2 downregulated cells compared to the controls in both the A2780 and ES2 cell lines (Figure 2A). Moreover, according to the influx and efflux curves, EZH2 depletion seemed to increase cellular platinum uptake rather than interfere with platinum efflux (Figure 2B,C). Furthermore, we used a fluorescence-modified cDDP analog, BODIPY-Pt, (Figure 2D) to track the process of cellular cDDP accumulation. Cells were transfected with non-fluorescently tagged siEZH2 to downregulate EZH2 expression (Figure 2E,F). Significant increases in intracellular BODIPY-Pt accumulation were observed in cells transfected with siEZH2 when compared with the controls, which was remarkably consistent with the results from the platinum accumulation assessment in cells exposed to cDDP (Figure 2G).

3.3 | Enhancer of zeste homolog 2 is involved in the interaction between cDDP and CTR1

Next, we observed an initial increase, followed by a decrease, in BODIPY-Pt in both the cells transfected with SiEZH2 and the control cells in a time-dependent manner, but there was a higher relative BODIPY-Pt

FIGURE 1 Enhancer of zeste homolog 2 (EZH2) expression is associated with cisplatin (cDDP) resistance in ovarian cancer cells and tumor tissue specimens. A, Representative images of immunohistochemical analysis of EZH2 (brown, nucleus) and copper transporter 1 (CTR1) (brown, cellular membrane) in ovarian cancer specimens (scale bar = 500 μm in 20× images; scale bar = 50 μm in 200×) and of the semiquantification of EZH2 and CTR1 expression in cDDP-sensitive/cDDP-resistant ovarian cancer specimens. Mann-Whitney test, $P = .0005$ and $P = .0007$. B, Colony formation assay and concentration survival curves for A2780, A2780C12, ES2, and ES2C12 cells after treatment with 2, 4, or 8 μmol/L cDDP (C12 cell lines were cDDP-resistant cells generated after 12 cycles of increasing cDDP exposure). C, Accumulation of EZH2 and H3K27Me3 during 1, 2, 4, 6, 9, and 12 cycles of increasing cDDP exposure in A2780 and ES2 cells as monitored by Western blot analysis. D,E, Western blot and quantitative real-time PCR analyses of EZH2 expression after transfection with EZH2 shRNA (ShEZH2) in A2780 and ES2 cells and EZH2 overexpressing plasmid in ES2 cells. F, Concentration survival curves for A2780 and ES2 cells incubated with serial doses of cDDP after EZH2 modification. Bars represent mean ± SD (n = 3). $^{*}P < .05$, $^{**}P < .01$, $^{***}P < .001$, $^{***}P < .0001$, Student's *t*-test. ShNC, scrambled control

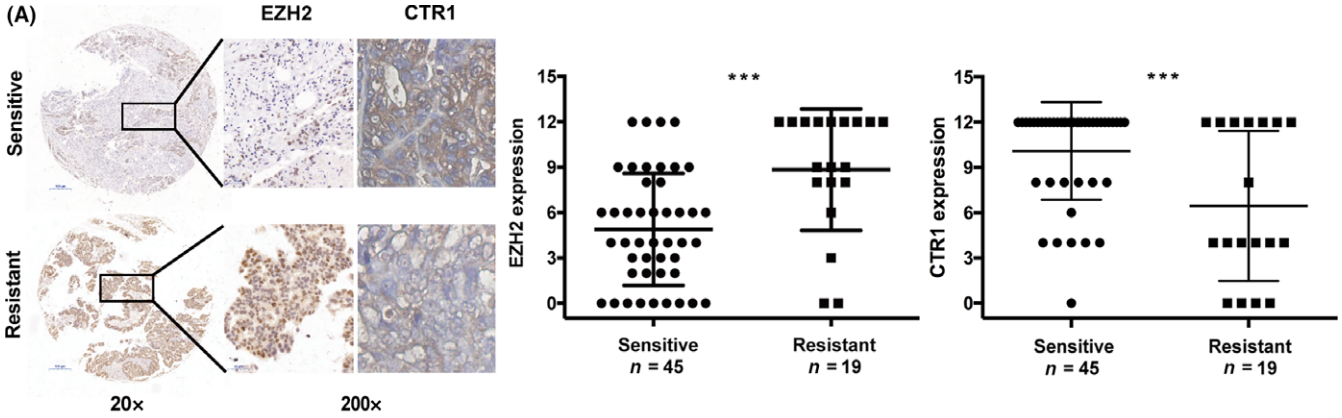
(A)
EZH2
CTR1
Sensitive
Resistant
20×
200×
EZH2 expression
CTR1 expression
***
Sensitive n = 45
Resistant n = 19

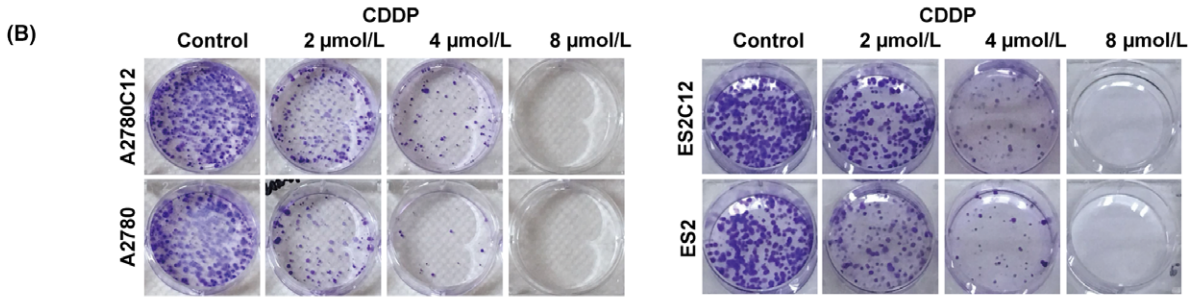
(B)
CDDP
Control
2 μmol/L
4 μmol/L
8 μmol/L
A2780C12
A2780
ES2C12
ES2

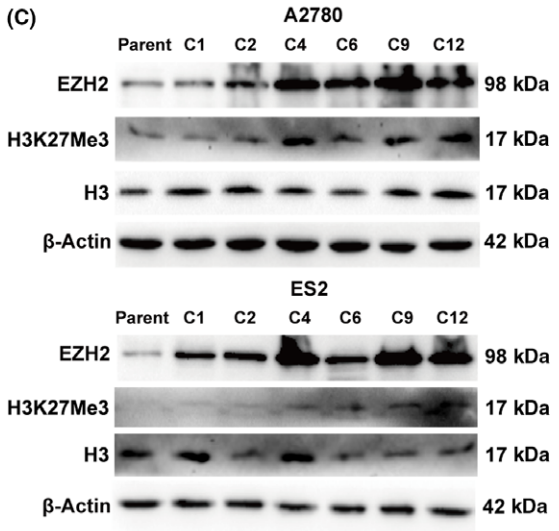
(C)
A2780
Parent C1 C2 C4 C6 C9 C12
EZH2
H3K27Me3
H3
β-Actin
98 kDa
17 kDa
42 kDa
ES2

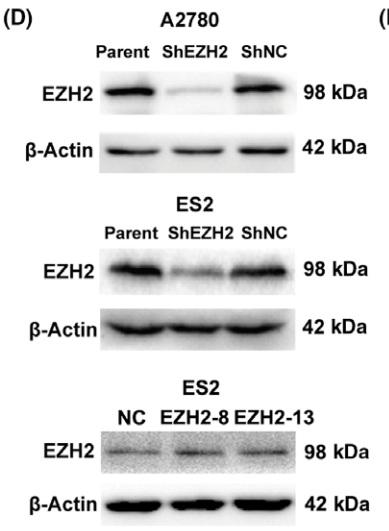
(D)
A2780
Parent ShEZH2 ShNC
EZH2
β-Actin
98 kDa
42 kDa
ES2
NC EZH2-8 EZH2-13

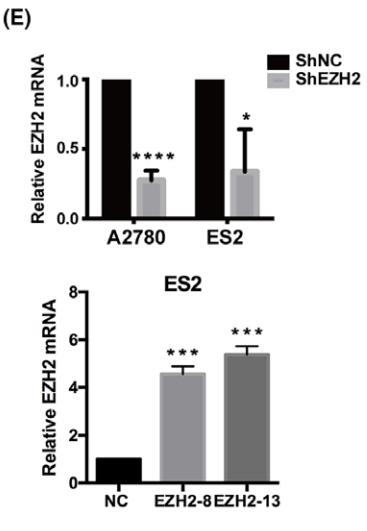
(E)
ShNC
ShEZH2
Relative EZH2 mRNA
A2780
ES2
NC
EZH2-8
EZH2-13

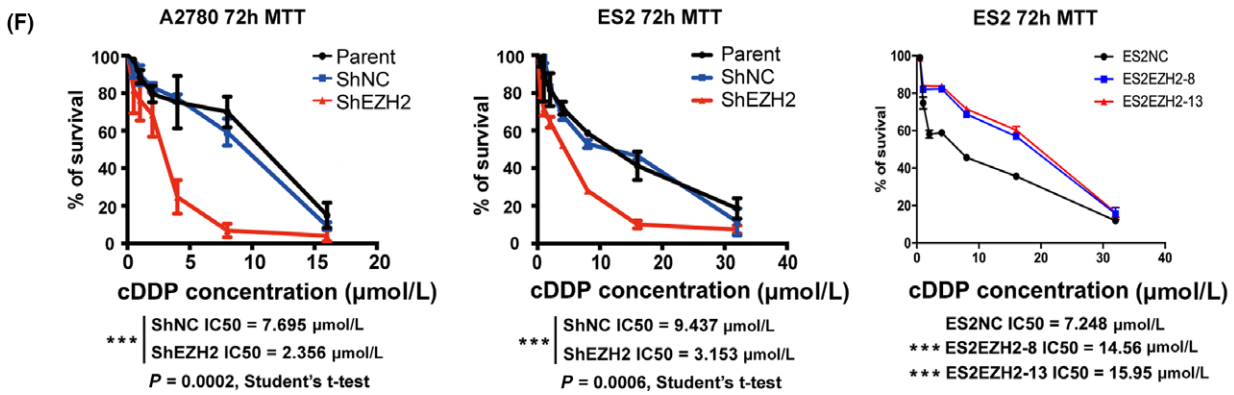
(F)
A2780 72h MTT
ES2 72h MTT
Parent
ShNC
ShEZH2
ES2NC
ES2EZH2-8
ES2EZH2-13
% of survival
cDDP concentration (μmol/L)
*** ShNC IC50 = 7.695 μmol/L
ShEZH2 IC50 = 2.356 μmol/L
P = 0.0002, Student's t-test
*** ShNC IC50 = 9.437 μmol/L
ShEZH2 IC50 = 3.153 μmol/L
P = 0.0006, Student's t-test
ES2NC IC50 = 7.248 μmol/L
*** ES2EZH2-8 IC50 = 14.56 μmol/L
*** ES2EZH2-13 IC50 = 15.95 μmol/L

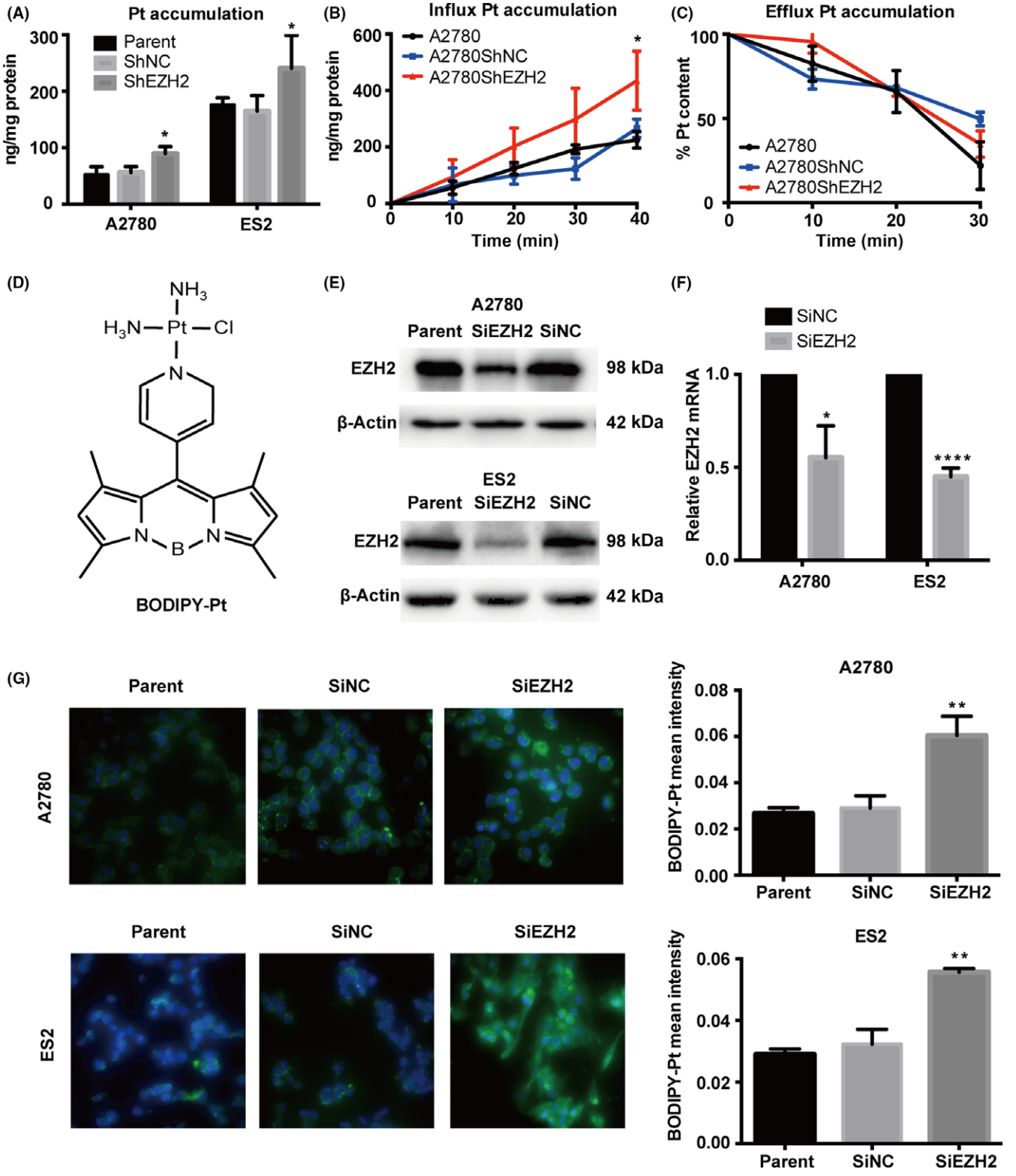

FIGURE 2 Enhancer of zeste homolog 2 (EZH2) expression is associated with cellular platinum accumulation. A, Cellular platinum (Pt) content of A2780 and ES2 cells with exposure to cisplatin (cDDP) after EZH2 depletion. B,C, Time course accumulation and efflux curve of cDDP in A2780 cells with cDDP exposure after EZH2 depletion. D, Chemical structure of the BODIPY-Pt complex. E,F, Western blot and quantitative real-time PCR analyses of EZH2 expression after transfection with EZH2 siRNA (SiEZH2) in A2780 and ES2 cells. G, Representative images of cellular BODIPY-Pt (green) merged with DAPI (blue) in A2780 and ES2 parent cells and in SiNC (Control) and SiEZH2 cells and the mean intensities of BODIPY-Pt in each cell line. Bars represent mean ± SD (n = 3). *$P < .05$, **$P < .01$, ****$P < .0001$, Student's *t*-test. ShEZH2, EZH2 shRNA; ShNC, scrambled control

intensity in the siEZH2 transfected cells (Figures 3A,S2). Previous studies reported that expression of the copper transporter CTR1 is closely related to cellular and tissue platinum accumulation and clinical outcomes.[18,20-22] In this case, we investigated cellular CTR1 expression and localization when treated with BODIPY-Pt. Cellular CTR1 expression (Figure 3A, red) underwent a minor decrease shortly after exposure to BODIPY-Pt and then remained steady (Figures 3A,S2). BODIPY-Pt (Figure 3A, green) had an early diffusion, and none entered the nucleus. A fraction of BODIPY-Pt remained at the surface of the cell during all time points, mirroring the CTR1 signal pattern. The Pearson correlation coefficients of the two signals were significant and consistent (Table S1). Given the involvement of EZH2 in cellular platinum accumulation and the engagement of CTR1 in transporting platinum complexes, we hypothesized that EZH2 might also play a role in the interaction between CTR1 and cDDP. Cellular CTR1 expression went through a time-dependent decrease when exposed to cDDP (Figure 3B) that was independent of drug concentration (Figure S2). Cisplatin caused greater CTR1 degradation in our previously generated cDDP-resistant cell line ACP when compared to A2780 (Figure 3C).[23] Next, we compared the response of CTR1 to cDDP when regulating EZH2 expression. We found that, after 12 hours of cDDP treatment, CTR1 expression decreased in the control cells but remained the same in EZH2 knockdown cells (Figure 3D). Similar results were seen when EZH2 was inhibited by GSK126 and DZNEP (Figure 3E).

3.4 | Enhancer of zeste homolog 2 accelerates cDDP-induced proteasomal CTR1 degradation

To explore further, we asked whether EZH2 has any influence on CTR1 protein stability. The half-life of CTR1 in cells transfected with shEZH2 and controls is similar (Figure 4A). Next, the cells were exposed to cDDP after cellular protein synthesis inhibition by CHX. EZH2 depletion protected CTR1 from cDDP-induced degradation (Figures 4B,S3). To confirm these results, we incubated the cells with MG132 to block the proteasomal degradation pathway mediated by ubiquitination and then measured the mono- and poly-ubiquitination level of CTR1 (Figure 4C). The mono- and poly-ubiquitinated CTR1 levels were significantly higher in controls than in cells transfected with shEZH2.

4 | DISCUSSION

In this study, we first established a significant association between EZH2 and cDDP resistance in the development of cellular cDDP-resistant models and the analysis of patient tissue samples. Then we examined the effect of EZH2 on cellular platinum accumulation directly by measuring cellular platinum content and indirectly by mimicking cDDP uptake with a fluorescence-conjugated platinum BODIPY-Pt; both methods showed that high EZH2 decreased cellular platinum uptake. Next, we found that EZH2 was somehow involved in the cDDP–CTR1 interaction and high EZH2 accelerated cDDP-induced proteasomal CTR1 degradation. These findings suggested that EZH2 plays a crucial role in the development of cDDP resistance.

Although it has been reported that the loss of EZH2 induces resistance to multiple drugs in acute myeloid leukemia,[24] we have collected several pieces of evidence showing that EZH2 plays a completely different role in ovarian cancer. We initially observed the correlation between EZH2 and cDDP resistance in a previously established pair of ovarian cancer cells, A2780 and A2780/DDP, in vitro and in vivo.[25] In our most recent generation of cDDP-resistant models, we not only obtained the same EZH2 expression pattern and biological cDDP reaction in the newly established cell line pairs A2780/A2780C12 and ES2/ES2C12 but also observed a cycle-by-cycle increase in EZH2 levels during repeated exposures to cDDP in the transition from parental to resistant cells. Similar results were also observed in SKOV3/SKOV3-3rd cells (resistant cell-line established from mouse s.c. xenografts of the third generation, three cycles of cDDP exposure per generation; data not shown). We further confirmed our findings using tissue samples from a cohort of patients. Other clinical evidence showed synthetic lethality for the use of an EZH2 inhibitor in SMARCA4-deficient ovarian small cell carcinomas, which suggested the possibility of combination treatment for overcoming cDDP resistance.[26] As EZH2 is the catalytic component of the PRC2, its classical function is to transfer methyl groups to histone 3 on lysine 27 by the SET domain to repress gene transcription in gene regulatory regions. In our previous work we found that EZH2-mediated H3K27 methylation contributed to cDDP resistance by increasing cellular proliferation.[25] However, we did not observe any cell proliferation increase in our current generated cell lines probably because that cellular growth was seriously impeded by the DNA lesions formed by repeated cycles of cDDP strikes. Yet the C12 cells still displayed cDDP resistance even without the characteristic of elevated cellular proliferation; therefore, we believed that, in addition to the EZH2/H3K27Me3 axis, there might be other mechanisms other than the classical PRC2 pathway through which EZH2 enhances cDDP resistance.

In addition to quantitative techniques for measuring intracellular platinum content, such as FAAS, inductively coupled plasma mass spectrometry, and mass cytometry, the application of fluorescently tagged mimics brought us one step closer to tracking the intracellular drug content. BODIPY-Pt is the platinum conjugate that bears characteristics most similar to cDDP: it is active against parental cells but less cytotoxic to resistant cells in both monolayer culture and spheroids, it produces DNA damage at a concentration approximately 1.5-fold its IC_{50} (the same as cDDP), and it accumulates less in cDDP-resistant cells compared to cDDP-sensitive cells.[27-29] Even with such promising attributes, we were fully aware that BODIPY-Pt might provide only limited information on the real fate of intracellular cDDP. Despite a preference for the mitochondria,[28] BODIPY-Pt was retained at the cell membrane much longer than expected, as evidenced by strong membrane signals observed even at later time points when overall intracellular intensity started to diminish. It is possible that this compound interacts with certain membrane proteins, such as a transporter.

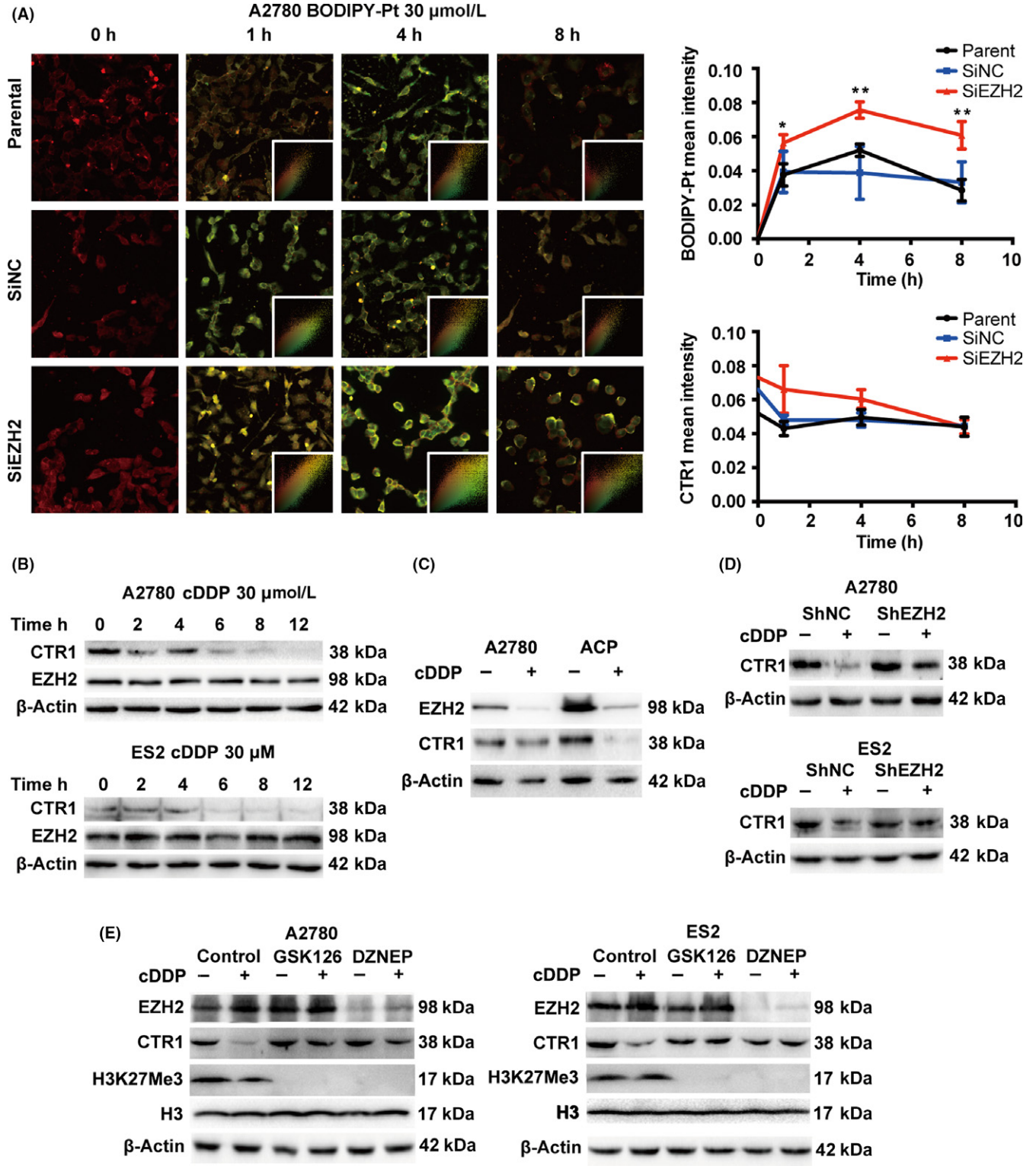

FIGURE 3 Enhancer of zeste homolog 2 (EZH2) is involved in the interaction between cisplatin (cDDP) and copper transporter 1 (CTR1). A, Representative images of cellular BODIPY-Pt accumulation (green) merged with CTR1 (red) in A2780SiEZH2, A2780SiNC, and A2780 cells treated with BODIPY-Pt and the mean intensities of BODIPY-Pt and CTR1 during the time course treatment. Bars represent the mean ± SD (n = 3). B, Western blot analysis for EZH2 and CTR1 in A2780 and ES2 cells receiving sequential cDDP treatment. C, Western blot analysis of EZH2 and CTR1 expression in a A2780 and ACP (a previously generated cDDP-resistant cell line) with the treatment of cDDP (30 μmol/L) for 12 h. D, Western blot analysis of EZH2 and CTR1 expression in A2780 and ES2 cells treated with EZH2 inhibitors GSK126 (2 μmol/L for 72 h) and 3-deazaneplanocin A DZNEP (2 μmol/L for 72 h) with the treatment of cDDP (30 μmol/L) for 12 h. E, Western blot analysis of EZH2 and CTR1 expression in A2780 and ES2 cells with scrambled control (shNC) or shEZH2 shRNA with the treatment of cDDP (30 μmol/L) for 12 h. *$P < .05$, **$P < .01$, Student's *t*-test

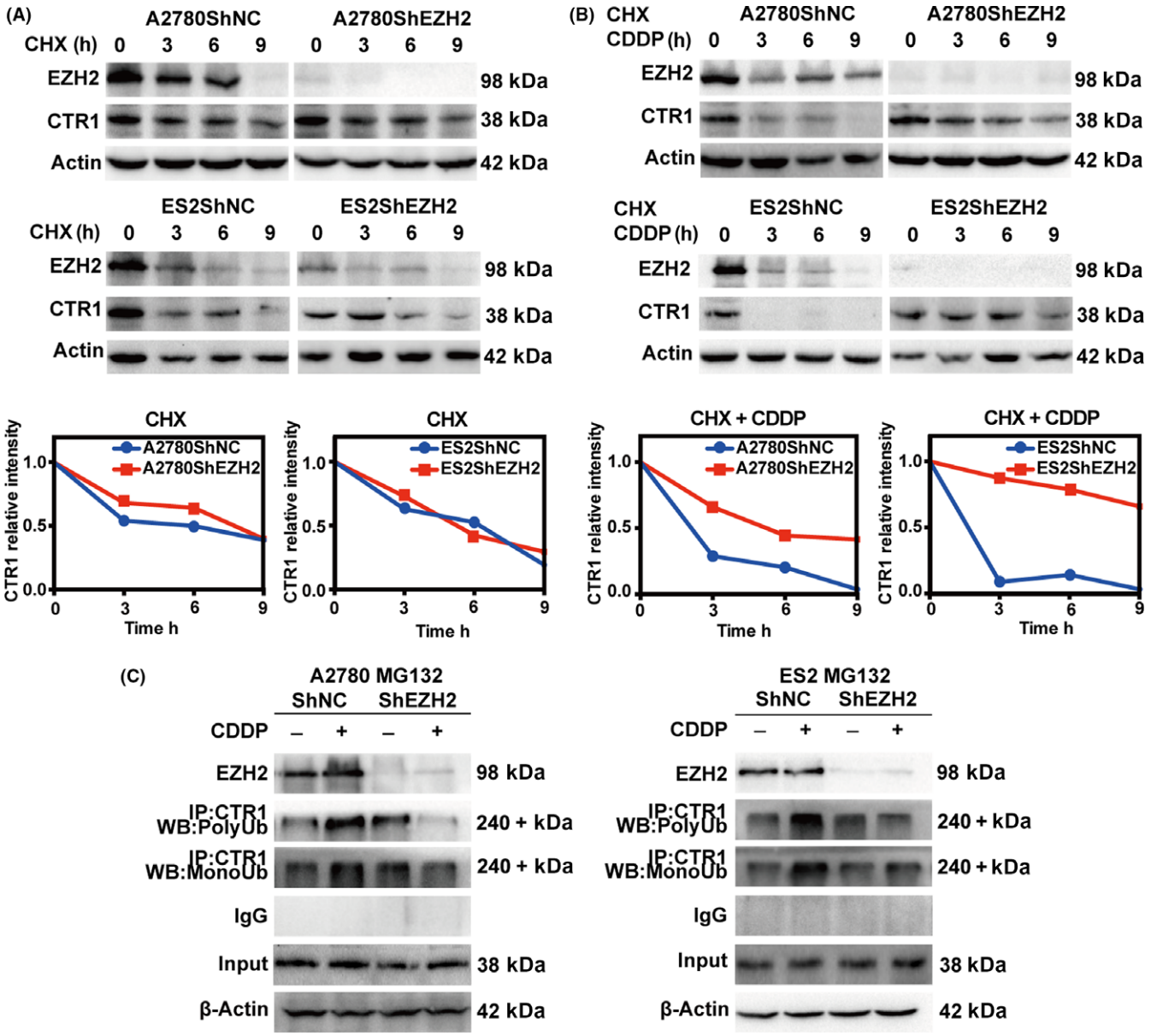

FIGURE 4 Enhancer of zeste homolog 2 (EZH2) is involved in cisplatin (cDDP)-induced proteasomal copper transporter 1 (CTR1) degradation. A, Western blot analysis for EZH2 and CTR1 in A2780ShNC, A2780ShEZH2, ES2ShNC, and ES2ShEZH2 cells treated with 20 μmol/L cycloheximide (CHX) for 3, 6, or 9 h and for the time course-incurred decrease in CTR1. B, Western blot analysis for EZH2 and CTR1 in A2780ShNC, A2780ShEZH2, ES2ShNC, and ES2ShEZH2 cells treated with 20 μmol/L CHX to block protein synthesis and then exposed to 30 μmol/L cDDP for 3, 6, or 9 h and the time course-incurred decrease in CTR1. C, Endogenous CTR1 immunoprecipitated from A2780ShNC, A2780ShEZH2, ES2ShNC, and ES2ShEZH2 cells treated with MG132, an inhibitor of the proteasomal degradation pathway, for 4 h and then treated with 30 μmol/L cDDP for 12 h. Western blot (WB) analysis of the mono-ubiquitination (MonoUb) and poly-ubiquitination (PolyUb) level of CTR1 in the immunoprecipitates

Several transporters are involved in platinum transportation including the copper transporting system and the organic cation transporters. We evaluated the prognostic implication of CTR1, CTR2, ATP7A, and ATP7B on ovarian cancer prognosis in our previous meta-analysis.[18] We only found correlation of clinical significance between chemotherapeutic resistance and CTR1 but not CTR2, ATP7A, or ATP7B. Additionally, we measured cellular ATP7A, ATP7B, and CTR2 expression after EZH2 modification by Western blot analysis, no significant changes were observed (Figure S4). Copper transporter 1 has gained much attention and raised furious debates ever since the discovery of its interaction with cDDP in yeast and mammals.[30,31] Based on current knowledge, the general role of CTR1, which was once proposed as a major pathway for cDDP uptake, must be re-evaluated due to various controversial results.[4,32-35] As the cellular expression level of CTR1 is significantly higher in sensitive cells than in resistant cells with matching cDDP uptake differences[32,34] and the tumor CTR1 level reportedly correlated with the prognosis in animal and clinical studies,[4,18,33,36] we

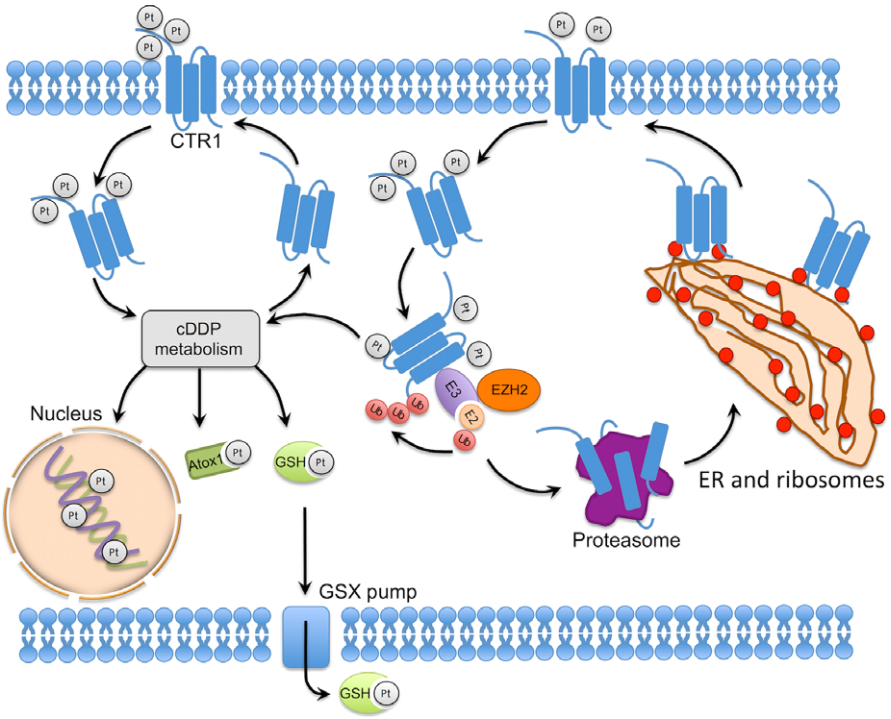

FIGURE 5 Proposed model for enhancer of zeste homolog 2 (EZH2) mediating cisplatin (cDDP)-induced copper transporter 1 (CTR1) degradation. Atox1, antioxidant 1 copper chaperone; ER, endoplasmic reticulum; E2, ubiquitin-conjugating enzyme; E3, ubiquitin ligase; GSH, Glutathione; GSX, glutathione S-conjugate; Pt, platinum; Ub, Ubiquitin

believed that CTR1 was still closely related to cDDP resistance. Cisplatin's ability to induce CTR1 degradation has been disputed for a long time.[37] Western blot analysis by Ivy et al and Akerfeldt et al[20,34] reported that the relationship between cDDP stimulation and CTR1 expression was irrelevant, whereas Holzer et al and Akerfeldt et al[20,38] observed a rapid downregulation of CTR1 in reaction to cDDP treatment. In agreement with the results reported by Wang et al,[35] we observed an overall CTR1 decrease at a much slower rate after cDDP treatment. Similar to the observation by Safaei et al,[39] the cDDP-induced CTR1 decrease was accompanied by an increase in CTR1 ubiquitination, a symbol of proteasomal degradation. The controversial results between these studies were probably due to variances in tumor type, detection methods, and reagent choice.

Based on our observation that depletion of EZH2 slowed cDDP-induced CTR1 degradation, we initially hypothesized that EZH2 might influence key enzymes regulating CTR1 degradation, as shown in Figure 5. In our attempt to identify key proteins contributing to CTR1 degradation, we pulled down CTR1-associated proteins by immunoprecipitation after cellular EZH2 modification. We submitted those CTR1-associated proteins for mass spectrometry analysis in order to find ubiquitin-associated proteins, which would likely be the targets of EZH2. However, like Tsai et al,[40] the E3 ligase of CTR1 was still not determined due to a noisy background created by cellular reactions to cDDP. Although we failed to tease out the CTR1-specific E3 ligase in cDDP-treated samples, we identified a series of depleted pathways for protein synthesis and metabolism (data not shown). A group of ribosome-associated proteins encoded by ribosome-related genes, once proposed to be involved in acquired cDDP resistance,[41] were depleted with EZH2 downregulation. It is still unclear how EZH2 contributes to cDDP-induced CTR1 degradation and whether the ribosome-related genes influenced by EZH2 play a role in acquired cDDP resistance. Although it is well recognized that EZH2 mainly located in the nuclei, several lines of evidence show that cytoplasmic EZH2 retains its methyl transfer activity and is involved in cellular skeleton movement, ubiquitin-mediated protein degradation, cytoskeleton formation, cell adhesion, and migration.[42-44] We examined the EZH2 location using immunofluorescence in several cell lines, including cDDP-sensitive/resistant cell lines and those with EZH2 depletion. We observed both nuclear and cytoplasmic EZH2 expression while EZH2 mainly remained in the nuclei. Based on previous findings, it is plausible that cytoplasmic EZH2 modulated CTR1 degradation through its methyl transfer activity.

In addition to mediating cellular platinum uptake, EZH2 participated in malignant biological behavior of ovarian cancer through regulating BRCA1 expression[15] and enhanced cDDP resistance through promoting DNA replication, pyrimidine metabolism, cell cycle, and cell proliferation.[25,45] Therefore, alteration of EZH2 regulating miRNAs and lncRNAs were also engaged in cDDP resistance.[46] All in all, the results of the current study provide new details regarding how EZH2 promotes platinum resistance by decreasing cellular platinum accumulation, which adds a new mechanism to the bulk repertoire; this mechanism can be applied when interpreting how EZH2 promotes malignancy and, more specifically, when determining the

unrecognized function of EZH2 that contributes to ovarian cancer platinum resistance.

ACKNOWLEDGMENTS

We thank all the patients who provided tissue samples, Dr. Wenliang Li for the preparation of BODIPY-Pt, and Dr. Yuzeng Zhang for FAAS technical support. This research was supported by the National Natural Science Foundation of China (No. 81572571 to JC, No. 81702570 to QY, and No. 81372807 to LY).

CONFLICT OF INTEREST

The authors have no conflict of interest.

ORCID

Zehua Wang http://orcid.org/0000-0001-6423-8219

REFERENCES

1. Beale PJ, Rogers P, Boxall F, Sharp SY, Kelland LR. BCL-2 family protein expression and platinum drug resistance in ovarian carcinoma. *Br J Cancer*. 2000;82:436-440.
2. Bogliolo S, Cassani C, Gardella B, et al. Oxaliplatin for the treatment of ovarian cancer. *Expert Opin Investig Drugs*. 2015;24:1275-1286.
3. Galluzzi L, Vitale I, Michels J, et al. Systems biology of cisplatin resistance: past, present and future. *Cell Death Dis*. 2014;5:e1257.
4. Ishida S, McCormick F, Smith-McCune K, Hanahan D. Enhancing tumor-specific uptake of the anticancer drug cisplatin with a copper chelator. *Cancer Cell*. 2010;17:574-583.
5. Kim ES, Tang X, Peterson DR, et al. Copper transporter CTR1 expression and tissue platinum concentration in non-small cell lung cancer. *Lung Cancer*. 2014;85:88-93.
6. Guancial EA, Kilari D, Xiao GQ, et al. Platinum concentration and pathologic response to cisplatin-based neoadjuvant chemotherapy in muscle-invasive bladder cancer. *PLoS ONE*. 2016;11:e0155503.
7. Cao R, Wang L, Wang H, et al. Role of histone H3 lysine 27 methylation in Polycomb-group silencing. *Science*. 2002;298:1039-1043.
8. Guo J, Cai J, Yu L, Tang H, Chen C, Wang Z. EZH2 regulates expression of p57 and contributes to progression of ovarian cancer in vitro and in vivo. *Cancer Sci*. 2011;102:530-539.
9. Yi X, Guo J, Guo J, et al. EZH2-mediated epigenetic silencing of TIMP2 promotes ovarian cancer migration and invasion. *Sci Rep*. 2017;7:3568.
10. Gui T, Bai H, Zeng J, et al. Tumor heterogeneity in the recurrence of epithelial ovarian cancer demonstrated by polycomb group proteins. *Onco Targets Ther*. 2014;7:1705-1716.
11. Fu Y, Chen J, Pang B, Li C, Zhao J, Shen K. EZH2-induced H3K27me3 is associated with epigenetic repression of the ARHI tumor-suppressor gene in ovarian cancer. *Cell Biochem Biophys*. 2015;71:105-112.
12. Xu L, Deng Q, Pan Y, et al. Cancer-associated fibroblasts enhance the migration ability of ovarian cancer cells by increasing EZH2 expression. *Int J Mol Med*. 2014;33:91-96.
13. Cardenas H, Zhao J, Vieth E, Nephew KP, Matei D. EZH2 inhibition promotes epithelial-to-mesenchymal transition in ovarian cancer cells. *Oncotarget*. 2016;7:84453-84467.
14. Xiao M, Cai J, Cai L, et al. Let-7e sensitizes epithelial ovarian cancer to cisplatin through repressing DNA double strand break repair. *J Ovarian Res*. 2017;10:24.
15. Li T, Cai J, Ding H, Xu L, Yang Q, Wang Z. EZH2 participates in malignant biological behavior of epithelial ovarian cancer through regulating the expression of BRCA1. *Cancer Biol Ther*. 2014;15:271-278.
16. Jia J, Zhang Y, Cai J, et al. A novel function of protein kinase B as an inducer of the mismatch repair gene hPMS2 degradation. *Cell Signal*. 2013;25:1498-1504.
17. Xiao M, Huang Z, Cai J, et al. Comparison of different sample preparation methods for platinum determination in cultured cells by graphite furnace atomic absorption spectrometry. *PeerJ*. 2017;5:e2873.
18. Sun S, Cai J, Yang Q, Zhao S, Wang Z. The association between copper transporters and the prognosis of cancer patients undergoing chemotherapy: a meta-analysis of literatures and datasets. *Oncotarget*. 2017;8:16036-16051.
19. Cai J, Yang C, Yang Q, et al. Deregulation of let-7e in epithelial ovarian cancer promotes the development of resistance to cisplatin. *Oncogenesis*. 2013;2:e75.
20. Akerfeldt MC, Tran CM, Shen C, Hambley TW, New EJ. Interactions of cisplatin and the copper transporter CTR1 in human colon cancer cells. *J Biol Inorg Chem*. 2017;22:765-774.
21. Safaei R, Adams PL, Maktabi MH, Mathews RA, Howell SB. The CXXC motifs in the metal binding domains are required for ATP7B to mediate resistance to cisplatin. *J Inorg Biochem*. 2012;110:8-17.
22. Tadini-Buoninsegni F, Bartolommei G, Moncelli MR, et al. Translocation of platinum anticancer drugs by human copper ATPases ATP7A and ATP7B. *Angew Chem*. 2014;53:1297-1301.
23. Yang C, Cai J, Wang Q, et al. Epigenetic silencing of miR-130b in ovarian cancer promotes the development of multidrug resistance by targeting colony-stimulating factor 1. *Gynecol Oncol*. 2012;124:325-334.
24. Gollner S, Oellerich T, Agrawal-Singh S, et al. Loss of the histone methyltransferase EZH2 induces resistance to multiple drugs in acute myeloid leukemia. *Nat Med*. 2017;23:69-78.
25. Hu S, Yu L, Li Z, et al. Overexpression of EZH2 contributes to acquired cisplatin resistance in ovarian cancer cells in vitro and in vivo. *Cancer Biol Ther*. 2010;10:788-795.
26. Morel D, Almouzni G, Soria JC, Postel-Vinay S. Targeting chromatin defects in selected solid tumors based on oncogene addiction, synthetic lethality and epigenetic antagonism. *Ann Oncol*. 2017;28:254-269.
27. Jagodinsky JC, Sulima A, Cao Y, et al. Evaluation of fluorophore-tethered platinum complexes to monitor the fate of cisplatin analogs. *J Biol Inorg Chem*. 2015;20:1081-1095.
28. Sun T, Guan X, Zheng M, Jing X, Xie Z. Mitochondria-Localized Fluorescent BODIPY-Platinum Conjugate. *ACS Med Chem Lett*. 2015;6:430-433.
29. Miller MA, Askevold B, Yang KS, Kohler RH, Weissleder R. Platinum compounds for high-resolution in vivo cancer imaging. *ChemMedChem*. 2014;9:1131-1135.
30. Ishida S, Lee J, Thiele DJ, Herskowitz I. Uptake of the anticancer drug cisplatin mediated by the copper transporter Ctr1 in yeast and mammals. *Proc Natl Acad Sci USA*. 2002;99:14298-14302.
31. Lin X, Okuda T, Holzer A, Howell SB. The copper transporter CTR1 regulates cisplatin uptake in Saccharomyces cerevisiae. *Mol Pharmacol*. 2002;62:1154-1159.
32. Zisowsky J, Koegel S, Leyers S, et al. Relevance of drug uptake and efflux for cisplatin sensitivity of tumor cells. *Biochem Pharmacol*. 2007;73:298-307.
33. Chen HH, Yan JJ, Chen WC, et al. Predictive and prognostic value of human copper transporter 1 (hCtr1) in patients with stage III non-

small-cell lung cancer receiving first-line platinum-based doublet chemotherapy. *Lung Cancer*. 2012;75:228-234.
34. Ivy KD, Kaplan JH. A re-evaluation of the role of hCTR1, the human high-affinity copper transporter, in platinum-drug entry into human cells. *Mol Pharmacol*. 2013;83:1237-1246.
35. Wang X, Jiang P, Wang P, Yang CS, Wang X, Feng Q. EGCG enhances cisplatin sensitivity by regulating expression of the copper and cisplatin influx transporter CTR1 in ovary cancer. *PLoS ONE*. 2015;10:e0125402.
36. Lee YY, Choi CH, Do IG, et al. Prognostic value of the copper transporters, CTR1 and CTR2, in patients with ovarian carcinoma receiving platinum-based chemotherapy. *Gynecol Oncol*. 2011;122:361-365.
37. Holzer AK, Samimi G, Katano K, et al. The copper influx transporter human copper transport protein 1 regulates the uptake of cisplatin in human ovarian carcinoma cells. *Mol Pharmacol*. 2004;66:817-823.
38. Holzer AK, Katano K, Klomp LW, Howell SB. Cisplatin rapidly down-regulates its own influx transporter hCTR1 in cultured human ovarian carcinoma cells. *Clin Cancer Res*. 2004;10:6744-6749.
39. Safaei R, Maktabi MH, Blair BG, Larson CA, Howell SB. Effects of the loss of Atox1 on the cellular pharmacology of cisplatin. *J Inorg Biochem*. 2009;103:333-341.
40. Tsai CY, Larson CA, Safaei R, Howell SB. Molecular modulation of the copper and cisplatin transport function of CTR1 and its interaction with IRS-4. *Biochem Pharmacol*. 2014;90:379-387.
41. Toshimitsu H, Hashimoto K, Tangoku A, et al. Molecular signature linked to acquired resistance to cisplatin in esophageal cancer cells. *Cancer Lett*. 2004;211:69-78.
42. Gunawan M, Venkatesan N, Loh JT, et al. The methyltransferase Ezh2 controls cell adhesion and migration through direct methylation of the extranuclear regulatory protein talin. *Nat Immunol*. 2015;16:505-516.
43. Chen R, Kong P, Zhang F, et al. EZH2-mediated alpha-actin methylation needs lncRNA TUG1, and promotes the cortex cytoskeleton formation in VSMCs. *Gene*. 2017;616:52-57.
44. Roy A, Basak NP, Banerjee S. Notch1 intracellular domain increases cytoplasmic EZH2 levels during early megakaryopoiesis. *Cell Death Dis*. 2012;3:e380.
45. Wang H, Yu Y, Chen C, et al. Involvement of enhancer of zeste homolog 2 in cisplatin-resistance in ovarian cancer cells by interacting with several genes. *Mol Med Rep*. 2015;12:2503-2510.
46. Liu L, Guo J, Yu L, et al. miR-101 regulates expression of EZH2 and contributes to progression of and cisplatin resistance in epithelial ovarian cancer. *Tumour Biol*. 2014;35:12619-12626.

SUPPORTING INFORMATION

Additional supporting information may be found online in the Supporting Information section at the end of the article.

How to cite this article: Sun S, Zhao S, Yang Q, et al. Enhancer of zeste homolog 2 promotes cisplatin resistance by reducing cellular platinum accumulation. *Cancer Sci*. 2018;109:1853–1864. https://doi.org/10.1111/cas.13599